The Journal of Experimental Biology 208, 3851-3858
Published by The Company of Biologists 2005
doi:10.1242/jeb.01848

Chloride turnover and ion-transporting activities of yolk-sac preparations (yolk balls) separated from Mozambique tilapia embryos and incubated in freshwater and seawater

Junya Hiroi[1,*], Hiroaki Miyazaki[2], Fumi Katoh[3], Ritsuko Ohtani-Kaneko[1] and Toyoji Kaneko[3]

[1]*Department of Anatomy, St Marianna University School of Medicine, Miyamae, Kawasaki 216-8511, Japan*, [2]*Department of Molecular Cell Biology, Graduate School of Medical Science, Kyoto Prefectural University of Medicine, Kamigyo, Kyoto 602-8566, Japan* and [3]*Department of Aquatic Bioscience, Graduate School of Agricultural and Life Sciences, University of Tokyo, Bunkyo, Tokyo 113-8657, Japan*

*Author for correspondence (e-mail: j-hiroi@marianna-u.ac.jp)

Accepted 14 August 2005

Summary

We have recently established a unique *in vitro* experimental model for mitochondrion-rich cell (MRC) research, a 'yolk-ball' incubation system, in which the yolk sac is separated from the embryonic body of Mozambique tilapia embryos and subjected to *in vitro* incubation. To evaluate the ion-transporting property of the yolk balls, we examined Cl^- content and turnover in yolk balls incubated in freshwater and seawater for 48 h, and distribution patterns of three ion transporters, Na^+/K^+-ATPase, $Na^+/K^+/2Cl^-$ cotransporter (NKCC) and cystic fibrosis transmembrane conductance regulator (CFTR), in MRCs in the yolk-sac membrane. The Cl^- turnover rate measured by whole-body influx of $^{36}Cl^-$ was about 60 times higher in yolk balls in seawater than in freshwater, while there was no essential difference in Cl^- content between them. Na^+/K^+-ATPase-immunoreactive MRCs were larger in yolk balls from seawater than yolk balls from freshwater. Distribution patterns of ion-transporting proteins allowed us to classify MRCs in freshwater yolk balls into three types: cells showing only basolateral Na^+/K^+-ATPase, cells showing basolateral Na^+/K^+-ATPase and apical NKCC, and cells showing basolateral Na^+/K^+-ATPase and basolateral NKCC. The seawater yolk balls, on the other hand, were characterized by the appearance of MRCs possessing basolateral Na^+/K^+-ATPase, basolateral NKCC and apical CFTR. Those seawater-type MRCs were considered to secrete Cl^- through the CFTR-positive apical opening to cope with diffusional Cl^- influx. These findings indicate that the yolk balls preserve the Cl^- transporting property of intact embryos, ensuring the propriety of the yolk ball as an *in vitro* experimental model for the yolk-sac membrane that contains MRCs.

Key words: yolk ball, mitochondrion-rich cell, tilapia, *Oreochromis mossambicus*, yolk-sac membrane, chloride, turnover.

Introduction

In teleosts, the gills, kidney and intestine are important osmoregulatory organs, creating ionic and osmotic gradients between the body fluid and external environments (Evans, 1993). Fish embryos and larvae also osmoregulate even though these osmoregulatory organs are not yet developed (Alderdice, 1988; Kaneko et al., 2002). In adult fish, mitochondrion-rich cells (MRCs, often referred to as chloride cells or ionocytes) are mostly located in the gills, functioning as the ion-secreting site in seawater fish and as the ion-absorbing site in freshwater fish. During early life stages of fish when functional gills are lacking, a rich population of MRCs is present in the yolk-sac membrane and other body surfaces, and those extrabranchial MRCs are the major ion-regulatory site in fish embryos (Kaneko et al., 2002).

Mozambique tilapia *Oreochromis mossambicus* is a euryhaline species that can mature and breed in both freshwater and seawater. The embryos are able to survive direct transfer from freshwater to seawater and *vice versa*, even though the developing gills are not functional (Ayson et al., 1994). Previous studies have demonstrated that MRCs located in the yolk-sac membrane are the extrabranchial site of ion exchange during the late embryonic stages of tilapia (Ayson et al., 1994, 1995; Shiraishi et al., 1997). MRCs in the yolk-sac membrane became larger and frequently formed multicellular complexes when embryos were transferred from freshwater to seawater, whereas small MRCs existed individually in freshwater (Shiraishi et al., 1997). Such cellular complexes, consisting of well-developed MRCs and accessory cells, are considered to be characteristic of seawater-type MRCs with ion-secreting functions (Kaneko and Shiraishi, 2001). Moreover, *in vivo* sequential observations on MRCs in the yolk-sac membrane have shown that small freshwater-type MRCs are transformed

into large seawater-type cells in response to seawater transfer, thus suggesting plasticity in ion-transporting functions of MRCs (Hiroi et al., 1999).

Using tilapia embryos, we have recently established a unique *in vitro* experimental model, a 'yolk-ball' incubation system, in which the yolk sac is separated from the embryonic body and subjected to *in vitro* incubation (Shiraishi et al., 2001). After appropriate cutting, the incision on the yolk ball healed during incubation in balanced salt solution (BSS), so that the yolk-sac membrane completely enclosed the yolk. Following transfer of the yolk balls prepared from freshwater tilapia embryos to seawater, MRCs formed new seawater-specific multicellular complexes together with accessory cells, as was observed in intact embryos transferred from freshwater to seawater. This indicates that MRCs are equipped with an autonomous mechanism of functional differentiation that is independent of embryonic endocrine and nervous systems.

The yolk-ball incubation system would serve as an excellent experimental model for further studies on MRC differentiation and functions. It is not clear, however, that the ion-transporting property of the yolk balls is comparable to that of intact embryos. In the present study, to evaluate the ion-transporting property of the yolk balls, we examined Cl^- content and turnover in the yolk balls incubated in freshwater and seawater. To further evaluate ion-transporting functions of MRCs in the yolk-sac membrane of the yolk balls, we investigated distributional patterns of three ion transporters: Na^+/K^+-ATPase, $Na^+/K^+/2Cl^-$ cotransporter (NKCC), and cystic fibrosis transmembrane conductance regulator (CFTR) that is considered to function as apical Cl^- channel (Marshall, 1995; Singer et al., 1998; McCormick et al., 2003). Our results indicated that the yolk balls preserved the Cl^- transporting property of intact embryos, and therefore help to justify the yolk ball as an *in vitro* experimental model for the yolk-sac membrane.

Materials and methods

Fish

Mozambique tilapia *Oreochromis mossambicus* Peters were maintained in tanks containing recirculating freshwater at 25°C. Fish were fed on artificial tilapia pellets (Tilapia 41M, Shikoku Kumiai Shiryo, Tokushima, Japan) once a day. Mature fish for breeding were kept in 200 l tanks to allow them to spawn, and fertilized eggs were collected from the mouth of brooding females 3 days after fertilization (2 days before hatching) for the preparation of yolk balls.

Preparation of yolk balls

The yolk balls were prepared according to Shiraishi et al. (2001). After removing the chorion, the embryo was placed in tilapia balanced salt solution (BSS: NaCl, 140 mmol l^{-1}; KCl, 3 mmol l^{-1}; $MgSO_4$, 1.25 mmol l^{-1}; NaH_2PO_4, 0.4 mmol l^{-1}; $NaHCO_3$, 2 mmol l^{-1}; $CaCl_2$, 1.5 mmol l^{-1}; Hepes, 10 mmol l^{-1}; penicillin, 100 U ml^{-1}; streptomycin, 0.1 mg ml^{-1}; pH 7.4). The yolk sac was then cut off from the embryonic body using sterilized fine scissors. When cut in a quick and smooth manner, the incision closed so that the yolk material did not leak through the incision. In cases where leakage of the yolk material was observed, the sample was discarded. After the surgical operation, the yolk ball was incubated at 25°C in BSS for 3 h to allow the wound to heal. The yolk-ball preparations were then incubated in freshwater (Na^+, 0.74 mmol l^{-1}; Ca^{2+}, 0.54 mmol l^{-1}; Mg^{2+}, 0.26 mmol l^{-1}; pH 7.0–7.5) or seawater (Na^+, 490 mmol l^{-1}; Ca^{2+}, 16 mmol l^{-1}; Mg^{2+}, 66 mmol l^{-1}; pH 7.5–8.1) for another 48 h. The incubation was conducted in tissue culture dishes (60 mm in diameter) containing 5 ml medium in an atmosphere of 100% air at 25°C.

Measurements of wet mass and chloride content

Wet mass of the individual yolk ball was measured to the nearest 0.1 mg after blotting on tissues. For the measurement of Cl^- content, 30 yolk balls were pooled and homogenized in 200 μl of distilled water. The homogenate was centrifuged at 18 000 ***g*** for 15 min, and Cl^- concentration of the supernatant was measured using a chloride meter (Buchler 4-2500, Fort Lee, NJ, USA), followed by calculation of Cl^- contents in the yolk balls. The chloride content was measured in triplicate for each experimental group. The data were expressed as the mean ± S.E.M. of total and mass-specific Cl^- contents.

Chloride turnover in the yolk ball

The rate of Cl^- uptake was measured by whole-body influx of $^{36}Cl^-$ as described previously (Miyazaki et al., 1998). Thirty yolk balls were placed in a beaker containing 15 ml of sterilized freshwater or seawater, and then $Na^{36}Cl$ (4.37 Mbq ml^{-1}, Amersham Biosciences, Uppsala, Sweden) was added to give a final specific activity of 60 kBq ml^{-1} (about 670 c.p.m. $nmol^{-1}$ Cl^- in freshwater and 2.5 c.p.m. $nmol^{-1}$ Cl^- in seawater). Changes in Cl^- levels of the bathing media were negligible. At 0.5, 1, 1.5, 2, 3 and 6 h after adding $Na^{36}Cl$, 5 yolk balls were removed from the beaker using a wide-mouthed pipette, expelled into a plastic dish and washed 5 times (1 min each) with 10 ml freshwater or seawater. The radioactivity of the third washing solution was not different from the background level. The samples were then placed in a miniature scintillation vial containing 1 ml of a solubilizing agent (Soluene-350, Packard, Meriden, CT, USA). When completely solubilized (24 h at 40°C), 3 ml scintillation fluid (Hionic Fluor, Packard) was added and radioactivity measured using a liquid scintillation counter (LS6000SC, Beckman, Fullerton, CA, USA).

Since the time course of $^{36}Cl^-$ influx was nonlinear, the rate of Cl^- influx was analyzed using a first-order rate equation as described by Brown and Tytler (1993): $Q=Q_{eq}(1–e^{–kt})$, where Q (c.p.m.) is the radioactivity at time t, Q_{eq} (c.p.m.) is the equilibration level of radioactivity, and k is the rate constant (turnover rate) of influx. The turnover rate was calculated by simple linear regression analysis of the plot of $\ln(Q_{eq}–Q)$ against t. The Q_{eq} (c.p.m. yolk $ball^{-1}$) of $^{36}Cl^-$ was estimated

by multiplying chloride content (nmol yolk ball^{-1}) by the specific activity of the external medium (cpm nmol^{-1}). The experiment was repeated three times, and the turnover rate was expressed as the mean ± S.E.M.

Triple-color whole-mount immunocytochemistry

To evaluate the ion-transporting function of MRCs, we examined distribution patterns of Na^+/K^+-ATPase, NKCC and CFTR within MRCs in the yolk-sac membrane according to the method reported by Hiroi et al. (2005). The antibody for Na^+/K^+-ATPase used here was raised against a synthetic peptide corresponding to a highly conserved region of the α-subunit of Na^+/K^+-ATPase, and has been proven to serve as a marker for MRCs (Uchida et al., 2000). The affinity-purified anti-Na^+/K^+-ATPase was conjugated to Alexa Fluor 546 (Katoh et al., 2003) using the Alexa Fluor Protein Labeling Kit (Molecular Probes, Eugene, OR, USA). The antibody to detect NKCC was a mouse monoclonal antibody directed against 310 amino acids at the carboxyl terminus of human colonic NKCC1 (T4, developed by Christian Lytle and Bliss Forbush III; obtained from the Developmental Studies Hybridoma Bank developed under the auspices of the National Institute of Child Health and Human Development and maintained by The University of Iowa, Department of Biological Sciences, Iowa City, IA, USA). The T4 antibody has been shown to be specifically immunoreactive to NKCC from many vertebrates including teleost fishes (Lytle et al., 1995; Wilson et al., 2000; Pelis et al., 2001; Marshall et al., 2002; McCormick et al., 2003; Wu et al., 2003; Hiroi et al., 2005). The antibody for CFTR was a mouse monoclonal antibody against 104 amino acids at the carboxyl terminus of human CFTR (R&D Systems, Boston, MA, USA). This antibody has also been shown to detect CFTR in some teleost species (Wilson et al., 2000; Marshall et al., 2002; Katoh and Kaneko, 2003; McCormick et al., 2003; Hiroi et al., 2005). To allow triple-color immunofluorescence staining, the mouse monoclonal antibodies against NKCC and CFTR were directly labeled with Alexa Fluor 647 and Alexa Fluor 488, respectively, using the Zenon Mouse IgG Labeling Kits (Molecular Probes).

The yolk balls were fixed in 4% paraformaldehyde in 0.1 mol l^{-1} phosphate buffer (pH 7.4) for 1 h, and then the yolk-sac membrane was carefully peeled off using sharp-pointed forceps. The membrane preparations were further fixed in the same fixative overnight, and preserved in 70% ethanol at 4°C. After a rinse with 0.01 mmol l^{-1} phosphate-buffered saline containing 0.2% Triton X-100 (PBST, pH 7.2) for 1 h, the fixed yolk-sac membrane was incubated simultaneously with Alexa-Fluor labeled anti-Na^+/K^+-ATPase, anti-NKCC and anti-CFTR for 12 h at 4°C. Anti-Na^+/K^+-ATPase was diluted 1:250, and anti-NKCC and anti-CFTR were used at concentrations of 0.8 μg ml^{-1} and 1.0 μg ml^{-1}, respectively. The antibodies were diluted with PBST containing 10% normal goat serum, 0.02% keyhole limpet hemocyanin, 0.1% bovine serum albumin and 0.01% sodium azide. The membrane was then washed in PBST for 1 h, subjected to post-staining fixation with 4% paraformaldehyde for 15 min, washed briefly in PBST, and mounted on a slide with Slow Fade Light (Molecular Probes). Confocal fluorescence images were taken using a Carl Zeiss 510 META confocal laser scanning microscope. The wavelengths of excitation and recorded emission for each Alexa dye are as follows: Alexa Flour 488, 488 nm and 505–530 nm; Alexa Fluor 546, 543 nm and 560–615 nm; and Alexa Fluor 647, 633 nm and 649–756 nm. To avoid any crosstalk, a 'multitrack' configuration was used, in which images were collected successively, rather than simultaneously, on three channels.

Scanning electron microscopic observations

To observe the apical structure of MRCs in the yolk-sac membrane, the yolk balls incubated in freshwater and seawater were fixed in 2% paraformaldehyde + 2% glutaraldehyde in 0.1 mol l^{-1} phosphate buffer (pH 7.4) overnight. Subsequently, the tissues were dehydrated in ethanol, transferred to 2-methyl-2-propanol, and dried using a freeze-drying device (JFD-300, JEOL, Tokyo, Japan). Dried samples were mounted on specimen stubs, coated with platinum palladium in an ion sputter (E-1030, Hitachi, Tokyo, Japan), and examined using a Hitachi S-4500 scanning electron microscope.

Statistics

The effect of incubation medium (preincubation in BSS, and 48-h incubation in freshwater and seawater) on wet mass of yolk balls was analyzed by a one-way analysis of variance (ANOVA) and the Tukey–Kramer *post hoc* test. No significant heterogeneity of variances was detected (the Bartlett's test, $P>0.05$). Significant differences in Cl^- content per ball, Cl^- content mg^{-1} mass and Cl^- turnover rates between freshwater and seawater groups were examined using the two-sample *t*-test. Data of Cl^- turnover rates that showed heterogeneity of variance were square-root-transformed before the *t*-test (Zar, 1999). All analyses were conducted using JMP 5.0.1 (SAS Institute, Cary, NC, USA) and $P<0.05$ was used to reject the null hypothesis.

Results

Wet mass, chloride content and chloride turnover rate

Representative pictures of yolk balls incubated in freshwater and seawater are shown in Fig. 1. Although yolk balls maintained their initial shape in both media after 48 h incubation, the average wet mass of yolk balls was significantly increased in freshwater and decreased in seawater, compared with those preincubated in BSS (Table 1; $P<0.05$, Tukey–Kramer *post hoc* test). There was a significant difference in mass between freshwater and seawater yolk balls ($P<0.05$, Tukey-Kramer *post hoc* test), as expected by their appearances (Fig. 1). The Cl^- contents and turnover rates were also compared between yolk balls incubated in freshwater and seawater (Table 1). There was no difference in either total or mass-specific Cl^- content between freshwater and seawater yolk balls. In contrast, the Cl^- turnover rates were markedly different between freshwater and seawater yolk balls. The

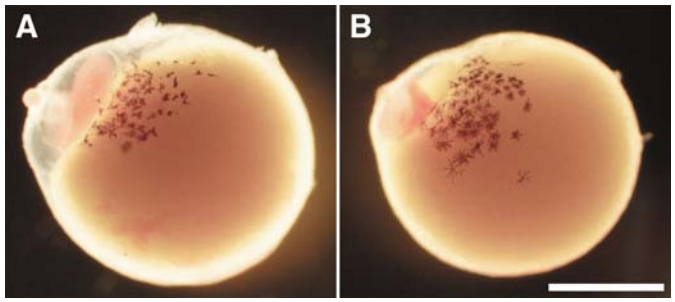

Fig. 1. Yolk balls prepared from Mozambique tilapia embryos and incubated in freshwater (A) and seawater (B) for 48 h. The yolk sac is completely enclosed by the yolk-sac membrane. The yolk balls slightly swelled in freshwater and shrunk in seawater. Bar, 200 μm.

Table 1. *Wet mass, Cl^- content and Cl^- turnover rate in yolk balls incubated in balanced salt solution for 3 h and those incubated in freshwater and seawater for another 48 h*

	BSS (0 h)	Freshwater (48 h)	Seawater (48 h)
Mass (mg)	4.6±0.1[a]	5.0±0.1[b]	4.1±0.2[c]
Total Cl^- content (μmol ball^{-1})	–	180±15	163±19
Mass-specific Cl^- content (μmol mg^{-1})	–	35.9±2.6	36.7±2.8
Cl^- turnover rate (% h^{-1})	–	0.003±0.001	0.167±0.033*

BSS, balanced salt solution.

[a,b,c]Different superscript letters indicate significant differences (P<0.05; Tukey–Kramer *post hoc* test).

*Significantly different from the values of freshwater yolk balls (P=0.0064; two-sample t-test).

turnover rate of seawater yolk balls was about 60 times higher than that of freshwater yolk balls.

Triple-color whole-mount immunocytochemistry

In the yolk-sac membrane of yolk balls incubated in freshwater, Na^+/K^+-ATPase-immunoreactive MRCs were round in shape and 10–25 μm in diameter (Fig. 2A). Although a minority of MRCs in yolk balls from seawater were of similar size and shape to MRCs from freshwater, the majority of MRCs in yolk balls from seawater were polygonal and 20–32 μm in diameter (Fig. 2E). In MRCs of both freshwater and seawater yolk balls, Na^+/K^+-ATPase immunoreactivity was detectable throughout the cell except for the nucleus and sub-apical region. Since it has been reported that Na^+/K^+-ATPase is present on both the basolateral membrane and the extensive tubular system that is continuous with the basolateral membrane of MRCs (Evans et al., 2005), the presence of Na^+/K^+-ATPase within MRCs represents their basolateral distribution.

Triple-color whole-mount immunocytochemistry clarified distribution patterns of Na^+/K^+-ATPase, NKCC and CFTR in MRCs in the yolk-sac membrane of freshwater (Fig. 2A–D) and seawater (Fig. 2E–H) yolk balls. In freshwater yolk balls, Na^+/K^+-ATPase-positive MRCs were classified into three types: cells showing only basolateral Na^+/K^+-ATPase (labeled as I in Fig. 2D), cells showing basolateral Na^+/K^+-ATPase and apical NKCC (II) and cells showing basolateral Na^+/K^+-ATPase and basolateral NKCC (III). Staining for

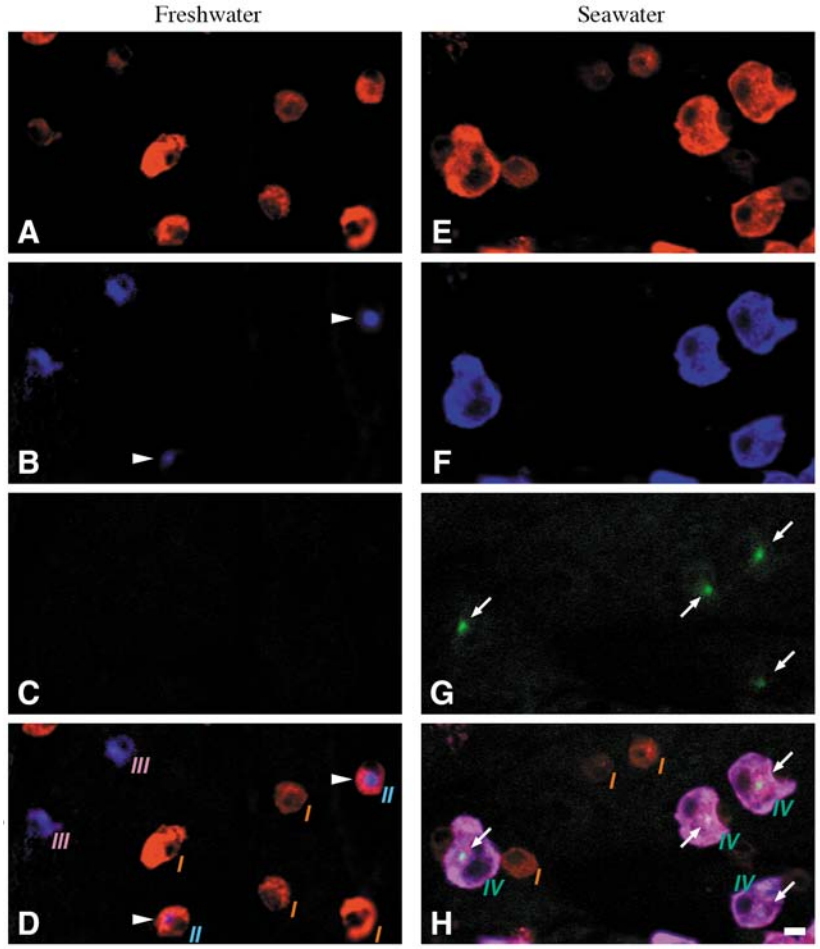

Fig. 2. Distribution patterns of ion-transporting proteins in mitochondrion-rich cells (MRCs) in the yolk-sac membrane of tilapia yolk balls incubated in freshwater (A–D) and seawater (E–H). The yolk-sac membranes were stained with anti-Na^+/K^+-ATPase (red; A,E), anti-$Na^+/K^+/2Cl^-$ cotransporter (NKCC) (blue; B,F), and anti-cystic fibrosis transmembrane conductance regulator (CFTR) (green; C,G). (D,H) Merged images of A–C (D) and E–G (H). Arrowheads and arrows indicate apical NKCC staining and apical CFTR staining, respectively. (I, II, III, IV) Functional classification of MRCs is based on distribution patterns of Na^+/K^+-ATPase, NKCC and CFTR, according to Hiroi et al. (2005). Scale bar, 10 μm.

CFTR was not detectable in MRCs in freshwater yolk balls. In seawater yolk balls, most of large MRCs showed basolateral Na^+/K^+-ATPase, basolateral NKCC and apical CFTR (IV in Fig. 2H). Small MRCs showed only basolateral Na^+/K^+-ATPase (I in Fig. 2H). A relatively small number of Na^+/K^+-ATPase-positive cells possessed only apical NKCC or only basolateral NKCC (not shown in Fig. 2H; similar to II or III in Fig. 2D).

Enlarged images of a MRC showing basolateral Na^+/K^+-ATPase and apical NKCC in a freshwater yolk ball (II in Fig. 2D), and basolateral Na^+/K^+-ATPase, basolateral NKCC and apical CFTR in a seawater yolk ball (IV in Fig. 2H) are shown in Figs 3 and 4, respectively. In the former, NKCC staining was concentrated at the apical region of the cell (Fig. 3C,D). In the latter, CFTR immunoreactivity was detectable at the apical region (Fig. 4E,F). NKCC staining was detectable throughout the cell except for the nucleus and CFTR-positive apical region, coinciding with the staining pattern of Na^+/K^+-ATPase (Fig. 4A–D). This cell type was accompanied by one or more accessory cells, forming a multicellular complex. The cytoplasm of the accessory cell was immunopositive for Na^+/K^+-ATPase but immunonegative for NKCC (Fig. 4A–D). Therefore, in the triple-color-merged images (Fig. 4G–I), the accessory cell remained in red, whereas the main MRC with red Na^+/K^+-ATPase and blue NKCC appeared in magenta.

Scanning electron microscopic observations

The apical openings of MRCs were observed by scanning electron microscopy (Fig. 5). In both freshwater and seawater yolk balls, most of the yolk-sac membrane was covered with pavement cells possessing arrays of microridges. The apical openings of MRCs were located at the boundary of the pavement cells. Although the apical membrane was

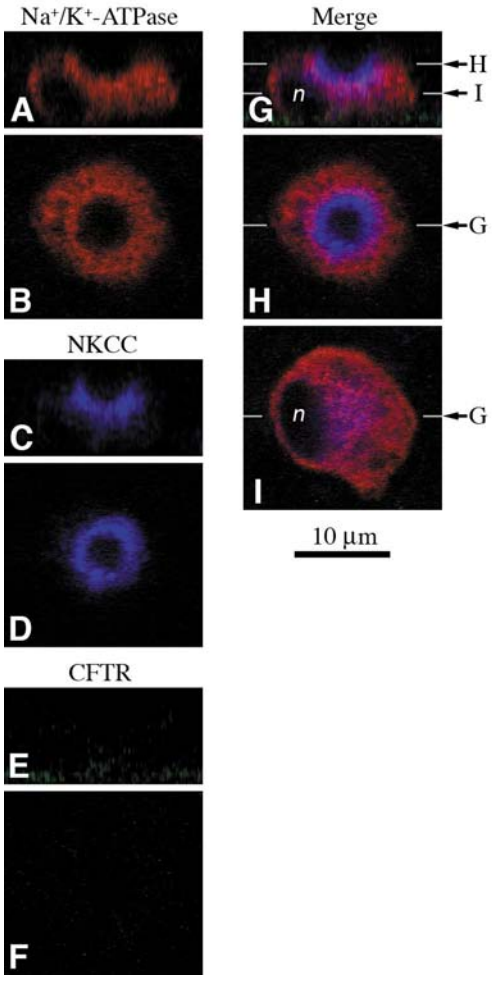

Fig. 3. Enlarged images of a typical mitochondrion-rich cell in freshwater yolk balls. (A,C,E,G) *X–Z* optical sections, cut transversely at the horizontal lines indicated in H and I. (B,D,F,H,I) *X–Y* optical sections, cut transversely at the lines indicated in G. n, nucleus. Scale bar, 10 μm.

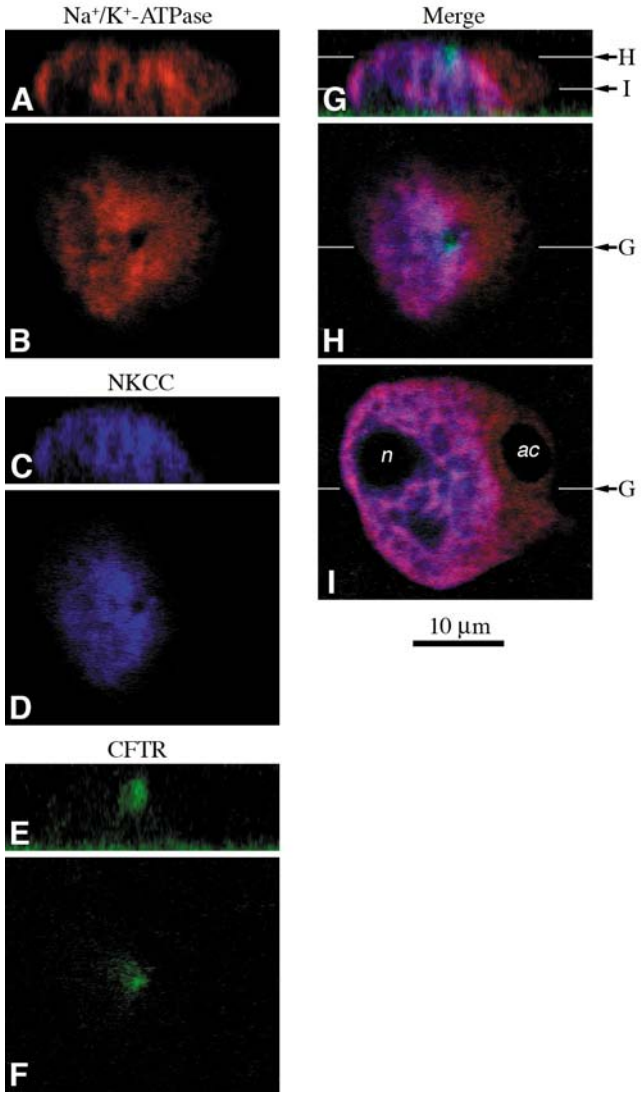

Fig. 4. Enlarged images of a typical mitochondrion-rich cell in seawater yolk balls. (A,C,E,G) *X–Z* optical sections. (B,D,F,H,I) *X–Y* optical sections. n, nucleus; ac, nucleus of accessory cell. Scale bar, 10 μm.

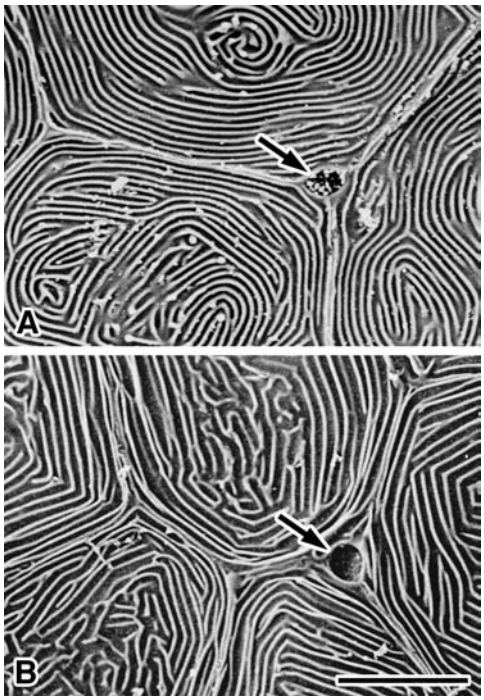

Fig. 5. Scanning electron micrographs of the yolk-sac membrane of tilapia yolk balls incubated in freshwater (A) and seawater (B) for 48 h. Apical openings (arrows) of mitochondrion-rich cells are located at the boundary of pavement cells possessing microridge structures. Scale bar, 10 μm.

invaginated to form apical crypts in both media, the apical openings were generally larger in seawater yolk balls than in freshwater ones. The apical membranes of MRCs were equipped with moderately developed microvilli in freshwater yolk balls (Fig. 5A), whereas such structures were not evident in the enlarged apical crypt in seawater (Fig. 5B).

Discussion

The yolk balls, preincubated in BSS for 3 h, swelled after 48 h incubation in freshwater, as shown by a slight increase in wet mass. Conversely, the yolk balls slightly shrank when incubated in seawater. As a result, yolk balls incubated in freshwater became significantly larger than those in seawater (Fig. 1, Table 1). Such changes in wet mass are thought to result from passive water movement down osmotic gradients between the internal fluid and external environments. Since the yolk balls completely lack any water regulatory organs such as kidney or intestine, they may not be able to regulate the volume of the internal fluid through active water transport. However, this is also the case with intact fish embryos, because of their incapacity for water extrusion as urine and for oral water uptake (Miyazaki et al., 1998). For instance, eyed-stage embryos of chum salmon *Oncorhynchus keta* shrink to some extent when transferred from freshwater to seawater (Kaneko et al., 1995). In general, water permeability is maintained extremely low during embryonic stages to avoid excess water movement (Guggino, 1980; Mangor-Jensen and Adoff, 1987; Miyazaki et al., 1998). In Mozambique tilapia acclimated to freshwater or seawater, it is reported that diffusional water permeability remains low during embryonic stages, but increases markedly after hatching (Miyazaki et al., 1998). In spite of slight expansion and shrinkage observed in freshwater and seawater, respectively, the yolk-sac membrane of the yolk balls seems to preserve the low water permeability of intact embryos, which minimizes passive water movements.

Cl^- concentration appears to be well regulated in the yolk balls, because total and mass-specific Cl^- contents showed no difference between freshwater and seawater yolk balls (Table 1). However, the Cl^- turnover rate measured by whole-body influx of $^{36}Cl^-$ was about 60 times higher in yolk balls in seawater than in freshwater (Table 1). The Cl^- turnover rates in the yolk balls are comparable to those measured in intact tilapia embryos (Miyazaki et al., 1998). The observation of similar Cl^- contents of yolk balls in seawater and freshwater suggests that the yolk balls possess mechanisms of Cl^- regulation, as is the case in intact embryos. In yolk balls incubated in seawater, where Cl^- permeability is greatly increased, it is inevitable that excess Cl^- be extruded in order to cope with diffusional Cl^- influx and maintain the Cl^- concentration in the physiological range. It would be reasonable to attribute active Cl^- secretion to MRCs, which are present in the yolk-sac membrane of tilapia embryos and larvae (Ayson et al., 1994; Shiraishi et al., 1997) as well as in that of yolk balls (Shiraishi et al., 2001).

On the basis of their morphology and responses to environmental salinity changes, branchial and extrabranchial MRCs in Mozambique tilapia have largely been classified into freshwater and seawater types (Ayson et al., 1994; Shiraishi et al., 1997; Hiroi et al., 1999; Uchida et al., 2000). The freshwater-type cells that are expected to absorb ions in hypoosmotic environments are small and located individually. Alternatively, the seawater-type cells, which seem to be responsible for ion secretion in hyperosmotic environments, are larger and indented by accessory cells to form multicellular complexes. In this study, the MRCs in yolk balls separated from embryos were also larger in seawater than freshwater (Fig. 2A,E) and were associated with accessory cells when incubated in seawater (Fig. 4G–I). Our scanning electron microscopic observations also showed a small apical pit of MRCs in freshwater yolk balls and an enlarged pit in seawater yolk balls (Fig. 5), which are characteristic of freshwater-type single MRCs and seawater-type multicellular complexes, respectively (Shiraishi et al., 1997). Such changes in MRC morphology are considered to reflect alteration in their ion-transporting functions. In fact, chloride test and X-ray microanalysis have shown that seawater-type MRC complexes have the definitive function of Cl^- secretion through enlarged apical pits, which was not observed in freshwater-type single MRCs (Kaneko and Shiraishi, 2001). Taken together, the current morphological observation on yolk ball MRCs in seawater are consistent with a function in Cl^- secretion.

The currently accepted model for NaCl secretion by MRCs

consists of the cooperative action of three major ion transporters: Na^+/K^+-ATPase, NKCC and CFTR (Marshall, 1995; McCormick et al., 2003). The Na^+/K^+-ATPase, which is localized to the basolateral membrane of MRCs, creates a low intracellular Na^+ concentration and negative charge within the cell. This Na^+ gradient drives transport of Na^+, K^+ and $2Cl^-$ into the cell through basolateral NKCC. Then, Cl^- leaves the cells down an electrical gradient through apical CFTR, whereas Na^+ is transported back outside the cells *via* Na^+/K^+-ATPase, and secreted by a paracellular pathway between chloride and accessory cells.

Based on three-dimensional distribution patterns of those three ion-transporting proteins within MRCs, we have recently reported functional classification of MRCs in the yolk-sac membrane of Mozambique tilapia embryos into four different types (Hiroi et al., 2005): type I, showing only basolateral Na^+/K^+-ATPase staining; type II, basolateral Na^+/K^+-ATPase and apical NKCC; type III, basolateral Na^+/K^+-ATPase and basolateral NKCC; and type IV, basolateral Na^+/K^+-ATPase, basolateral NKCC and apical CFTR. Type-II cells seemingly correspond to 'freshwater-type' ion-absorptive MRCs, since the cell types were not found in seawater but appeared and increased in number after transfer from seawater to freshwater. In contrast, type-IV cells may represents 'seawater-type' ion-secretory MRCs, because the cells were not observable in freshwater but rapidly appeared following transfer from freshwater to seawater.

In the present triple-color whole-mount immunocytochemistry, types I, II and III MRCs were identified in freshwater yolk balls (Fig. 2D). It is likely that freshwater yolk balls preserved the MRC populations of the intact embryos that had been kept in freshwater, being favorable for freshwater acclimation. Alternatively, the yolk balls incubated in seawater were characterized by the predominant occurrence of type-IV cells with basolateral Na^+/K^+-ATPase, basolateral NKCC and apical CFTR. The intracellular localization of those three proteins within type-IV cells is completely consistent with the current accepted model for ion secretion by MRCs, and the predominant occurrence of type-IV cells can account for active ion secretion in seawater yolk balls.

Type-IV MRCs were not observable in intact embryos reared in freshwater, but rapidly appeared following transfer from freshwater to seawater; these type-IV cells were previously thought to originate mostly from pre-existing type-I cells and type-III cells (Hiroi et al., 2005). Type-IV cells observed in seawater yolk balls are also considered to develop from pre-existing type-I and type-III cells after exposure to seawater. This conversion of MRC types in the yolk-sac membrane of yolk balls, which reflects changes in the expression and localization of ion transport proteins, is likely to be independent of the embryonic endocrine and nervous systems. Similarly, it has been demonstrated in killifish that seawater-type MRCs are transformed into freshwater-type cells as a short-term response to transfer from seawater to freshwater, followed by the promotion of MRC replacement as a long-term response (Katoh and Kaneko, 2003).

Although we did not address Na^+ permeability in yolk balls, Na^+ influx is expected to be higher in seawater than in freshwater, as seen in Cl^- permeability. Occurrence of Na^+/K^+-ATPase in the basolateral membrane of type-IV MRCs in seawater yolk balls implies a Na^+-secreting function. This is also supported by the formation of multicellular complexes consisting of type-IV and accessory cells, presumably providing a paracellular pathway for Na^+ secretion (Shiraishi et al., 1997).

In vitro experimental models have been used for MRC research in the past, such as primary cultures of gill epithelial cells (Battram et al., 1991; Perry and Walsh, 1989; Pärt and Bergström, 1995; Avella and Ehrenfeld, 1997; Wood and Pärt, 1997), and opercular and yolk-sac membrane preparations (Karnaky et al., 1977; McCormick, 1990; Marshall, 1995; Ayson et al., 1995). The yolk-ball incubation system that we have established has the following advantages over the conventional *in vitro* experimental models: (1) the tissue including MRCs can survive for a long period, so that the morphological alteration of MRCs can be followed; (2) MRCs maintain the ability of cellular differentiation; (3) the tissue preparation is free from the embryonic endocrine and nerve systems; and (4) the cellular polarity can be maintained and the serosal side of the yolk-sac membrane is separated from the external environment (Shiraishi et al., 2001). In addition, the present study has demonstrated that the yolk ball preserves the Cl^- transporting properties of the intact embryo, presumably because the yolk-ball incubation system utilizes the intact yolk-sac membrane of tilapia embryos without cellular reconstitution. These findings help establish the isolated yolk ball as an *in vitro* experimental model for the yolk-sac membrane containing MRCs. The ion-absorptive functions by freshwater-type MRCs are currently less well understood than seawater-type ion-secretory MRCs (Perry 1997; Evans et al., 2005). In addition to molecular cloning and immunocytochemical studies on ion transporters that could be involved in ion uptake from freshwater, such as vacuolar-type H^+ ATPase, Na^+ channel, Na^+/H^+ exchanger and NKCC, yolk balls are expected to serve as a suitable model to examine the ion-uptake functions of these transporters.

References

Alderdice, D. F. (1988). Osmotic and ionic regulation in teleost eggs and larvae. In *Fish Physiology*, Vol. XIA (ed. W. S. Hoar and D. J. Randall), pp. 163-251. San Diego, California: Academic Press.

Avella, M. and Ehrenfeld, J. (1997). Fish gill respiratory cells in culture: a new model for Cl^- secreting epithelia. *J. Membr. Biol.* **156**, 87-97.

Ayson, F. G., Kaneko, T., Hasegawa, S. and Hirano, T. (1994). Development of mitochondrion-rich cells in the yolk-sac membrane of embryos and larvae of tilapia, *Oreochromis mossambicus*, in fresh water and seawater. *J. Exp. Zool.* **270**, 129-135.

Ayson, F. G., Kaneko, T., Hasegawa, S. and Hirano, T. (1995). Cortisol stimulates the size and number of mitochondrion-rich cells in the yolk-sac membrane of embryos and larvae of tilapia (*Oreochromis mossambicus*) *in vitro* and *in vivo*. *J. Exp. Zool.* **272**, 419-425.

Battram, J. C., Eddy, F. B., Chang, Y. J. and Filder, J. (1991). Chloride transport by isolated gill cells of the fresh water adapted rainbow trout (*Salmo gairdneri*). *Comp. Biochem. Physiol.* **94**A, 439-445.

Brown, J. A. and Tytler, P. (1993). Hypoosmoregulation of larvae of the

turbot, *Scophthalamus maximus*: drinking and gut function in relation to environmental salinity. *Fish Physiol. Biochem.* **10**, 475-483.

Evans, D. H. (1993). Osmotic and ionic regulation. In *The Physiology of Fishes* (ed. D. H. Evans), pp. 315-341. Boca Raton, Florida: CRC Press.

Evans, D. H., Piermarini, P. M. and Choe, K. P. (2005). The multifunctional fish gill: dominant site of gas exchange, osmoregulation, acid-base regulation, and excretion of nitrogenous waste. *Physiol. Rev.* **85**, 97-177.

Guggino, W. B. (1980). Water balance in embryos of *Fundulus heteroclitus* and *F. bermudae* in seawater. *Am. J. Physiol.* **238**, R36-R41.

Hiroi, J., Kaneko, T. and Tanaka, M. (1999). *In vitro* sequential changes in chloride cell morphology in the yolk-sac membrane of Mozambique tilapia (*Oreochromis mossambicus*) embryos and larvae during seawater adaptation. *J. Exp. Biol.* **202**, 3485-3495.

Hiroi, J., McCormick, S. D., Ohtani-Kaneko, R. and Kaneko, T. (2005). Functional classification of mitochondrion-rich cells in euryhaline Mozambique tilapia (*Oreochromis mossambicus*) embryos, by means of triple immunofluorescence staining for Na^+/K^+-ATPase, $Na^+/K^+/2Cl^-$ cotransporter and CFTR anion channel. *J. Exp. Biol.* **208**, 2023-2036.

Kaneko, T. and Shiraishi, K. (2001). Evidence for chloride secretion from chloride cells in the yolk-sac membrane of Mozambique tilapia larvae adapted to seawater. *Fish Sci.* **67**, 541-543.

Kaneko, T., Hasegawa, S., Takagi, Y., Tagawa, M. and Hirano, T. (1995). Hypoosmoregulatory ability of eyed-stage embryos of chum salmon. *Mar. Biol*. **122**, 165-170.

Kaneko, T., Shiraishi, K., Katoh, F., Hasegawa, S. and Hiroi, J. (2002). Chloride cells in early life stages of fish and their functional differentiation. *Fish Sci.* **68**, 1-9.

Karnaky, K. J., Jr, Degnan, K. J. and Zadunaisky, J. A. (1977). Chloride transport across isolated opercular epithelium of killifish: a membrane rich in chloride cells. *Science* **195**, 203-205.

Katoh, F. and Kaneko, T. (2003). Short-term transformation and long-term replacement of branchial chloride cells in killifish transferred from seawater to freshwater, revealed by morphofunctional observations and a newly established 'time-differential double fluorescent staining' technique. *J. Exp. Biol.* **206**, 4113-4123.

Lytle, C., Xu, J. C., Biemesderfer, D. and Forbush, B., III (1995). Distribution and diversity of Na-K-Cl cotransport proteins: a study with monoclonal antibodies. *Am. J. Physiol.* **269**, C1496-C1505.

Mangor-Jensen, A. and Adoff, G. R. (1987). Drinking activity of the newly hatched larvae of cod (*Gadus morhua* L.). *Fish Physiol. Biochem.* **3**, 99-103.

Marshall, W. S. (1995). Transport processes in isolated teleost epithelia: Opercular epithelium and urinary bladder. In *Cellular and Molecular Approaches to Fish Ionic Regulation* (ed. C. M. Wood and T. J. Shuttleworth), pp. 1-23. San Diego, California: Academic Press.

Marshall, W. S., Lynch, E. M. and Cozzi, R. R. (2002). Redistribution of immunofluorescence of CFTR anion channel and NKCC cotransporter in chloride cells during adaptation of the killifish *Fundulus heteroclitus* to sea water. *J. Exp. Biol.* **205**, 1265-1273.

McCormick, S. D. (1990). Cortisol directly stimulates differentiation of chloride cells in tilapia opercular membrane. *Am. J. Physiol.* **259**, R857-R863.

McCormick, S. D., Sundell, K., Bjornsson, B. T., Brown, C. L. and Hiroi, J. (2003). Influence of salinity on the localization of Na^+/K^+-ATPase, $Na^+/K^+/2Cl^-$ cotransporter (NKCC) and CFTR anion channel in chloride cells of the Hawaiian goby (*Stenogobius hawaiiensis*). *J. Exp. Biol.* **206**, 4575-4583.

Miyazaki, H., Kaneko, T., Hasegawa, S. and Hirano, T. (1998). Developmental changes in drinking rate and ion and water permeability during early life stages of euryhaline tilapia, *Oreochromis mossambicus*, reared in fresh water and seawater. *Fish Physiol. Biochem*. **18**, 277-284.

Pärt, P. and Bergström, E. (1995). Primary cultures of teleost branchial epithelial cells. In *Cellular and Molecular Approaches to Fish Ionic Regulation* (ed. C. M. Wood and T. J. Shuttleworth), pp. 207-227. San Diego, California: Academic Press.

Pelis, R. M., Zydlewski, J. and McCormick, S. D. (2001). Gill Na^+-K^+-$2Cl^-$ cotransporter abundance and location in Atlantic salmon: effects of seawater and smolting. *Am. J. Physiol.* **280**, R1844-R1852.

Perry, S. F. (1997). The chloride cell: structure and function in the gills of freshwater fishes. *Annu. Rev. Physiol.* **59**, 325-347.

Perry, S. F. and Walsh, P. J. (1989). Metabolism of isolated fish cells: contribution of epithelial chloride cells. *J. Exp. Biol.* **144**, 507-520.

Shiraishi, K., Kaneko, T., Hasegawa, S. and Hirano, T. (1997). Development of multicellular complexes of chloride cells in the yolk-sac membrane of tilapia (*Oreochromis mossambicus*) embryos and larvae in seawater. *Cell Tissue Res.* **288**, 583-590.

Shiraishi, K., Hiroi, J., Kaneko, T., Matsuda, M., Hirano, T. and Mori, T. (2001). *In vitro* effects of environmental salinity and cortisol on chloride cell differentiation in embryos of Mozambique tilapia, *Oreochromis mossambicus*, measured using a newly developed 'yolk-ball' incubation system. *J. Exp. Biol.* **204**, 1883-1888.

Singer, T. D., Tucker, S. J., Marshall, W. S. and Higgins, C. F. (1998). A divergent CFTR homologue: highly regulated salt transport in the euryhaline teleost *F. heteroclitus*. *Am. J. Physiol.* **274**, C715-C723.

Uchida, K., Kaneko, T., Miyazaki, H., Hasegawa, S. and Hirano, T. (2000). Excellent salinity tolerance of Mozambique tilapia (*Oreochromis mossambicus*): Elevated chloride cell activity in the branchial and opercular epithelia of the fish adapted to concentrated seawater. *Zool. Sci.* **17**, 149-160.

Wilson, J. M., Randall, D. J., Donowitz, M., Vogl, A. W. and Ip, A. K. (2000). Immunolocalization of ion-transport proteins to branchial epithelium mitochondria-rich cells in the mudskipper (*Periophthalmodon schlosseri*). *J. Exp. Biol.* **203**, 2297-2310.

Wood, C. M. and Pärt, P. (1997). Cultured branchial epithelia from freshwater fish gills. *J. Exp. Biol.* **200**, 1047-1059.

Wu, Y. C., Lin, L. Y. and Lee, T. H. (2003). Na^+,K^+,$2Cl^-$ cotransporter: a novel marker for identifying freshwater- and seawater-type mitochondria-rich cells in gills of the euryhaline tilapia, *Oreochromis mossambicus*. *Zool. Stud.* **42**, 186-192.

Zar, J. H. (1999). *Biostatistical Analysis*, 4th edn. Upper Saddle River, New Jersey: Prentice-Hall.